

pubs.acs.org/jasms Article

Standards-Free Absolute Quantitation of Oxidizable Glycopeptides by Coulometric Mass Spectrometry

Kai-Yuan Chiu, Yongling Ai, Md Tanim-AI Hassan, Xuanwen Li, Harsha P. Gunawardena,* and Hao Chen*



Cite This: J. Am. Soc. Mass Spectrom. 2024, 35, 1441-1450



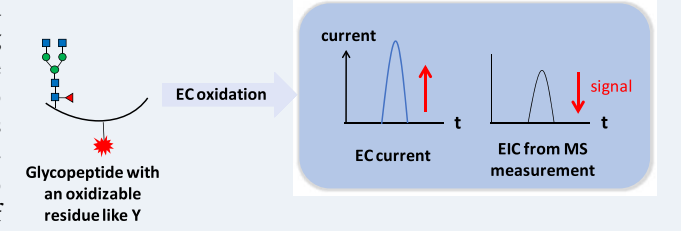
ACCESS I

III Metrics & More

Article Recommendations

Supporting Information

ABSTRACT: Currently, glycopeptide quantitation is mainly based on relative quantitation due to absolute quantitation requiring isotope-labeled or standard glycopeptides which may not be commercially available or are very costly and time consuming to synthesize. To address this grand challenge, coulometric mass spectrometry (CMS), based on the combination of electrochemistry (EC) and mass spectrometry (MS), was utilized to quantify electrochemically active glycopeptides without the need of using standard materials. In this study, we studied tyrosine-



containing glycopeptides, NYIVGQPSS(β -GlcNAc)TGNL-OH and NYSVPSS(β -GlcNAc)TGNL-OH, and successfully quantified them directly with CMS with a discrepancy of less than 5% between the CMS measured amount and the theoretical amount. Taking one step further, we applied this approach to quantify glycopeptides generated from the digestion of NIST mAb, a monoclonal antibody reference material. Through HILIC column separation, five N297 glycopeptides resulting from NIST mAb tryptic digestion were successfully separated and quantified by CMS for an absolute amount without the use of any standard materials. This study indicates the potential utility of CMS for quantitative proteomics research.

KEYWORDS: absolute quantitation, glycopeptide, antibody, mass spectrometry, electrochemistry

■ INTRODUCTION

Post-translational modifications (PTMs) are chemical modifications of proteins following RNA translation. PTMs increase the functional diversity of the proteome and influence many aspects of cell biology. Glycosylation is considered as one of the most complex PTMs and is critical for the functions and characteristics of proteins, such as their conformation, stability, distribution,² pharmacokinetic and pharmacodynamic properties, 3,4 and protease resistance. 5 Over the past decade, research has revealed that glycosylation is important for cell signaling, 6-8 vaccine development, 9,10 cellular control of diabetes, 11-13 and cancers. 14-17 For instance, aberrant glycosylation of immunoglobulin is linked to disease activity and pathogenesis. 18 Glycosylation typically found in the fragment crystallizable (Fc) region is essential for the activation of downstream effector functions of immunoglobulin G (IgG)⁶ and therefore crucial for the development of therapeutic recombinant IgG antibodies. As the research focus of glycoproteomics has expanded from glycan profiling to site occupancy 19-21 and expression levels, 22-24 there is an urgent need for accurate and robust site-specific glycans and glycopeptide quantitation.

Recent advances in instrumentation, ^{25,26} sample preparation techniques ^{27–29} and enrichment strategies ^{30–34} have fortified MS-based glycoproteomics in more advanced applications. The most common approach for quantifying glycans or glycopeptides is based on relative quantitation. Novel chemical labeling

strategies are employed to overcome the limits of low abundance within proteolytic mixtures and poor ionization efficiency of glycosylated species encountered in traditional methods.³⁵ Stable isotopic labeling,³⁶ isobaric labeling,³⁷ metabolic incorporation,³⁸ label-free enzymatic reactions,³⁹ and multiple reaction monitoring (MRM) methods⁴⁰ have been developed for glycopeptide quantitative analysis. Glycoforms are typically measured by normalizing the signal strengths to examine quantitative changes at a site-specific level. 41,42 However, the difference in ionization efficiency and fragmentation efficiency between different glycoforms might greatly impact the normalized ion abundances, thus leading to inaccurate results. 43 Absolute quantitation involving isotope labeling and internal standards provides more robust, reliable, and precise quantitative results, which helps in understanding patient-centric product development. However, syntheses of those standard compounds can face multiple challenges including the high cost of labor and time. In addition, the isotope-labeled glycopeptide standards are often unavailable. 41,44 Recently, two-dimensional

 Received:
 February 12, 2024

 Revised:
 May 7, 2024

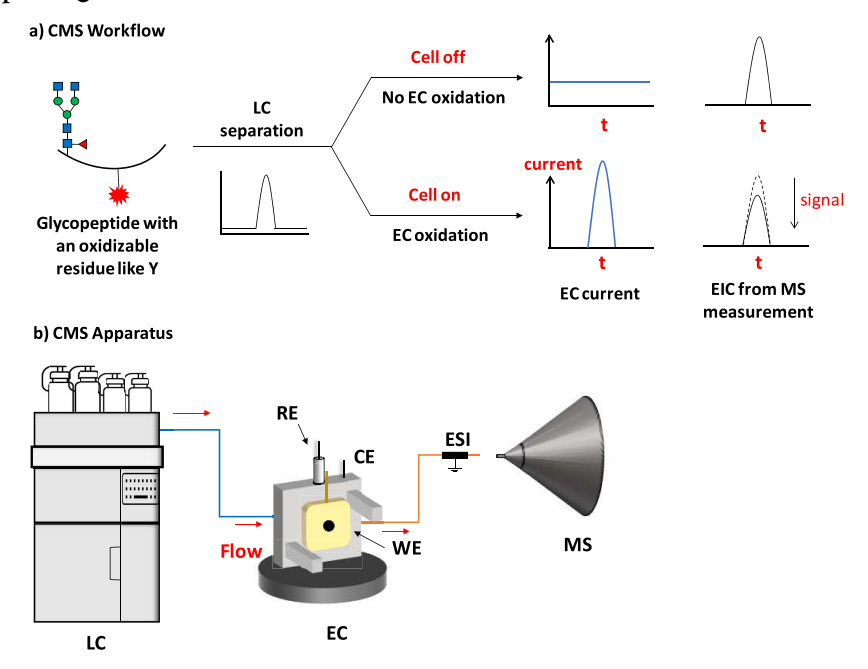
 Accepted:
 May 13, 2024

 Published:
 May 30, 2024





Scheme 1. (a) Workflow for Quantitation of Tyrosine-Containing Glycopeptides; (b) Schematic Showing the LC/EC/MS Apparatus for Glycopeptide Quantitation (b)



"Glycopeptides are first separated through LC and then oxidized in an electrochemical flow cell to collect the electrochemical oxidation current. MS is used to monitor the signal change of glycopeptides upon oxidation (note that the peptide signal drops due to oxidative consumption as illustrated). BRE, reference electrode; CE, counter electrode; WE, working electrode.

chromatographic separation was used to purify and gain IgG-1 glycopeptides from digestion, which were used as standards for glycopeptide quantitation.⁴⁵ However, this purification process and subsequent characterization of the purified glycopeptides took time. Therefore, there is a pressing need to develop an absolute quantitation method for glycopeptides without using standards.

In this study, we present a coulometric mass spectrometric (CMS) method for absolute quantitation of oxidizable glycopeptides. As glycopeptides are generated from enzymatic digestion of glycoproteins, this method also provides a new way to quantify glycoproteins. Our CMS method does not require the use of standards or isotope-labeled glycopeptides to achieve absolute quantitation. As illustrated in Scheme 1a, if a target glycopeptide contains an oxidizable residue like tyrosine or tryptophan, it can be introduced by liquid chromatography (LC) to an electrochemical flow cell for electrochemical oxidation, followed by MS detection. The recorded electric current response can be integrated over time to calculate the total electric charge (Q) involved in oxidation, which is related to the amount of oxidized glycopeptide. According to the Faraday's law, Q is proportional to the quantity of the oxidized glycopeptide: Q = nzF, where n is the number moles of oxidized glycopeptide, z is the number of electrons transferred per molecule during the redox reaction (e.g., z = 2 for oxidation of tyrosine residue), and F is the Faraday constant $(9.65 \times 10^4 \text{ C/})$ mol). Upon electrochemical oxidation, the glycopeptide shows a reduced MS intensity. From the relative change of the target glycopeptides peak area in the extracted ion chromatogram (EIC) before and after electrolysis, the oxidation yield Δi can be calculated. The moles of oxidized glycopeptide in combination with the oxidation yield can be used to calculate the total amount of the glycopeptide analyte, which is $n/\Delta i = (Q/zF)/\Delta i = Q/zF$ $(zF\Delta i)$.

Previously, we have established that the CMS method can be used for accurately quantifying small-molecule organic molecules (e.g., uric acid, N-nitrosamine), tyrosine- or tryptophan-containing peptides, and large-molecule proteins. $^{46-54}$ In this study, we applied the method for absolute quantitation of glycopeptides. By using our approach, we successfully quantified the absolute amounts of glycopeptides NYIVGQPSS(β -GlcNAc)TGNL and NYSVPSS(β -GlcNAc)TGNL. The amount measured by CMS is in excellent agreement with the theoretical value (measurement error of <5%). In addition, by quantifying the surrogate glycopeptides released from trypsin digestion of NIST mAb, we showed that antibody glycosylation can be quantified with our method as well.

■ EXPERIMENTAL SECTION

Chemicals. Xyloglucan heptasaccharide, 6^3 , 6^4 - α -D-galactosyl-mannopentaose, 2^3 -(4-O-methyl- α -D-glucuronosyl)-xylotetraose, 6^3 - α -D-glucosyl-maltotriosyl-maltotriose, and 2^3 , 3^3 -di- α -L-arabinofuranosyl-xylotriose were obtained from Megazyme (Bray, Ireland). H-Ser(β -GlcNAc)-OH, SVES(β -GlcNAc)-GSADAK-NH₂, NYIVGQPSS(β -GlcNAc)TGNL-OH, and NYSVPSS(β-GlcNAc)TGNL-OH (HPLC grade) were purchased from Sussex Research (ON, Canada). HPLC-grade acetonitrile, formic acid, and 1 M Tris-HCl buffer solution (pH 7.0) were from Fisher Scientific (Waltham, MA). Humanized IgG1 κ monoclonal antibody (mAb, NIST reference material 8671, 10 mg/mL) was purchased from NIST. N-Acetyl-Dglucosamine (β -GlcNAc), urea, dithiothreitol (DTT), iodoacetamide (IAA), and calcium chloride were purchased from Sigma-Aldrich (St. Louis, MO). Sequencing-grade trypsin was obtained from Roche (GmbH, Mannheim, Germany). Deionized water used for sample preparation was obtained using a Millipore Direct-Q5 purification system (Burlington,

MA). A PD spin trap G-25 column for desalting was obtained from Cytiva (Marlborough, MA).

Instrumentation. Scheme 1b illustrates the experimental setup of coulometric mass spectrometry (CMS) consisting of an ultraperformance liquid chromatography system (UPLC, Waters, Milford, MA) coupled with an electrochemical thinlayer flow cell (BASi, West Lafayette, IN; cell dead volume ca. 1 μL) and a high-resolution Orbitrap Q Exactive mass spectrometer (Thermo Scientific, San Jose, CA). The electrochemical cell was equipped with an 8 mm i.d. boron-doped diamond (BDD, Fraunhofer USA, Inc., MI) disc as the working electrode (WE) and an Ag/AgCl reference electrode (RE), and the cell stainless steel body served as a counter electrode (CE, catalog no. MF1092). An electrochemical analyzer (BASi, West Lafayette, IN) was used to monitor and record the oxidation current. The electric current peak was integrated with OriginPro 2018b software to calculate the total electric charge of Q. The eluent flowing out of electrochemical cell was analyzed using online electrospray ionization mass spectrometry (ESI-MS). The applied ionization voltage and the flow rate of the nitrogen sheath gas were +4 kV and 10 L/h, respectively. The ion transfer inlet capillary temperature was kept at 250 °C. Mass spectra were acquired by Thermo Xcalibur (3.0.63).

Antibody Digestion. A 200 μ g amount of NIST mAb was denatured using 80 μ L of 8 M urea at room temperature followed by reduction with 2.5 μ L of 1 M DTT at 37 °C for 1 h. Next, alkylation was performed by adding 10 μ L of 500 mM IAA at room temperature in the dark for 30 min. The sample mixture was then desalted by a PD SpinTrap G-25 column (the column was equilibrated with calcium chloride buffer) before being subjected to digestion by adding 10 μ L of trypsin (1 μ g/ μ L) (1:20 enzyme:protein ratio, w/w) at 37 °C overnight. Approximately 130 μ L of acetonitrile was added to the digested sample to make up 250 μ L of total volume. The final IgG concentration was 0.8 μ g/ μ L.

LC/EC/MS Analysis. For standard glycopeptides, a reversed phase column (BEH C18, 2.1 mm \times 100 mm, 1.7 μ m; Waters Corp., Milford, MA) was used for UPLC separation. The gradient program was as follows (min/% B): 0/95, 5/5, 10/95. Mobile phase A was 0.1% formic acid in water; mobile phase B was 0.1% formic acid in acetonitrile; flow rate = 200 μ L/min; injection volume = 3 μ L; column temperature = 20 °C. A potential of +1.05 V (vs Ag/AgCl) was applied to the WE to trigger the oxidation of LC-separated glycopeptides.

The digested NIST mAb was separated by a HALO penta-HILIC column (2.1 mm \times 250 mm; 2.7 μm particle size; Advanced Materials Technology, Wilmington, DE). The mobile phase flow rate was 200 $\mu L/min$. The following gradient (min/% B) was used: 0/90, 10/80, 35/65, 40/40, 45/40, 48/80, 60/90. Mobile phase A was 0.1% formic acid in water; mobile phase B was 0.1% formic acid in acetonitrile. The injection volume was 10 μL , and column temperature was kept at 40 °C. A potential of +1.2 V (vs Ag/AgCl) was applied to the WE to trigger the oxidation of LC-separated glycopeptides.

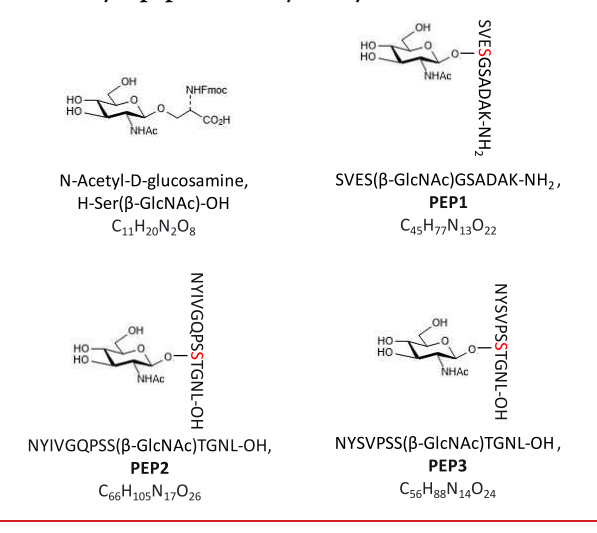
■ RESULTS AND DISCUSSION

Investigation of Glycan and Glycopeptide Oxidation Under CMS Conditions. Electrochemical detection of glycans using a gold electrode under alkaline pH (pH 10) has been well documented in the literature. Typically, the oxidation of glycans results in the aldehyde functional group being converted into carboxylic acid. However, in our CMS experiment which utilized the LC/EC/MS setup, an acidic pH and organic solvent

additives are used to assist LC separation of peptides and MS detection; we thus first examined whether or not glycans can be still oxidized under our LC/EC/MS conditions. In this study, we tested six glycans, N-acetyl-D-glucosamine, xyloglucan heptasaccharide, 2³-(4-O-methyl-α-D-glucuronosyl)-xylotetraose, 2^3 , 3^3 -di- α -L-arabinofuranosyl-xylotriose, 6^3 - α -D-glucosyl-maltotriosyl-maltotriose, and 6^3 , 6^4 - α -D-galactosyl-mannopentaose, with the applied potential at 1.05 V (vs Ag/AgCl). All of these glycans have terminal aldehyde groups of different sizes (Scheme S1, Supporting Information). Each glycan was prepared in 0.1% formic acid in water to 500 μ M and injected by LC into the electrochemical cell with an injection volume of 3 μ L at a flow rate of 200 μ L/min. No oxidation product as well as no oxidation current was detected by MS for all of these six glycans (Figure S1, Supporting Information). It appears that electrochemical oxidation of glycans does not occur under the acidic LC conditions with the BDD electrode that we used (1.05 V vs Ag/AgCl).

Next, we examined an amino acid and a peptide carrying a GlcNAc glycan, H-Ser(GlcNAc- β -D)-OH, and SVES(β -GlcNAc)GSADAK-NH₂ (PEP1) (Scheme 2) under the same

Scheme 2. Structures and Chemical Formulas of Glycoamino Acid and Glycopeptides Analyzed by CMS



oxidation conditions as the glycan oxidation experiments described above. Again, no oxidation product was detected by MS, and no oxidation current was observed by potentiostat for the glycoamino acid (Figure S2, Supporting Information). Small amounts of oxidized product were detected for PEP1 probably due to in-source oxidation; no additional product or oxidation current was observed when applying the potential (Figure S3, Supporting Information). It appears that electrochemical oxidation of glycans does not occur under the acidic LC conditions with our BDD electrode.

Absolute Quantitation of Oxidizable Glycopeptides by CMS. When glycopeptides have an oxidizable residue such as tyrosine, electric oxidation current can be observed (e.g., see data below in Figure 1) and they could be quantified by our CMS method. Two tyrosine-containing glycopeptides NYIVGQPSS(β-GlcNAc)TGNL-OH (PEP2) and NYSVPSS-(β-GlcNAc)TGNL-OH (PEP3) were chosen as test samples for CMS quantitation (Scheme 2). PEP2 contains an O-GlcNAcylation site on its second serine residue. In our experiment, 3 μL of 25 μM PEP2 was injected by LC (injected

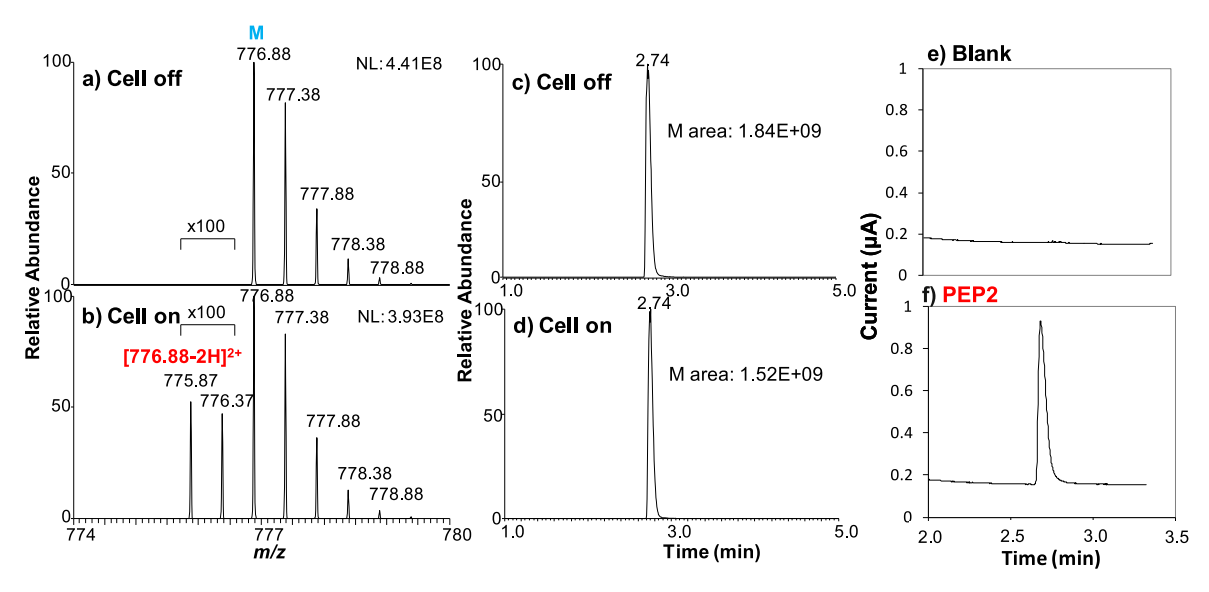
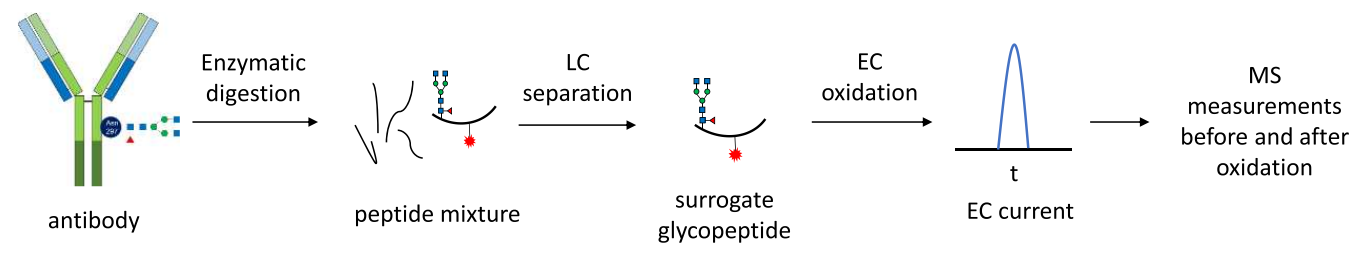


Figure 1. ESI-MS spectra of NYIVGQPSS(β -GlcNAc)TGNL (PEP2) when the applied potentials are (a) 0 and (b) +1.05 V. The major peak of the oxidized product of PEP2 was seen at m/z 775.87 (+2 charge) in b. EICs of the +2 charge of the PEP2 ion (m/z 776.88) recorded when the applied potentials are (c) 0 and (d) +1.05 V. Electric current responses are shown (e) from the blank solvent and (f) from the oxidation of PEP2.

Scheme 3. Schematic Showing the CMS Workflow for Absolute Antibody Quantitation



* An oxidizable amino acid residue such as Y

amount 75 pmol) for electrolysis in the cell. Before electrolysis (with a 0 V oxidation potential), a +2 ion of **PEP2** at m/z 776.9 was observed (Figure 1a). After electrolysis (with a 1.05 V oxidation potential), the +2 ion of the oxidized glycopeptide product was observed at m/z 775.9 (Figure 1b), corresponding to the oxidation product ion by loss of two hydrogens and two electrons from PEP2 via electrolysis. The observed peptide product ion has a reduced mass by 2 Da in comparison to the intact peptide ion, which is in agreement with the fact that the tyrosine residue would lose two hydrogens and two electrons (i.e., z = 2) to convert its phenol group to a semiquinone moiety upon electrochemical oxidation. 46 Indeed, no electrochemical current was observed for various aforementioned glycans, H-Ser(GlcNAc-β-D)-OH and SVES(β-GlcNAc)GSADAK-NH₂ which lack a Y residue. Figure 1c and 1d shows the EICs of m/z 776.9 before and after electrolysis. By comparing the EIC signal change, the oxidation yield was obtained to be 17.5% (Table S1, Supporting Information). Note that as the third isotopic peak of m/z 775.9 would overlap with the peak of m/z776.9, we corrected the EIC peak areas of m/z 776.9 for the oxidation yield calculation by subtracting the contribution of the third isotope peak of m/z 775.9 to the EIC peak area of m/z776.9. The contribution of the third isotope peak of m/z 775.9 to the EIC peak area of m/z 776.9 can be calculated based on an EIC peak area of m/z 775.9 and the observed peak ratio between the first and the third isotopic peaks of m/z 776.9 (i.e.,

correction factor α = 0.35, Table S1, Supporting Information). Meanwhile, an electric current peak was detected for PEP2, as shown in Figure 1f. A blank solvent was injected under the same oxidation conditions as a control to show the background current as seen in Figure 1e. No electric current peak was observed for the solvent, suggesting that the electric current detected in Figure 1f was caused by the oxidation of glycopeptides PEP2. Based on the integration of the glycopeptide current peak area, according to Faraday's law, the amount of the oxidized PEP2 was calculated to be 14.0 pmol (Table S1, Supporting Information). In consideration of the oxidation yield of 17.5%, the measured amount of PEP2 was 75.5 pmol. This experiment was performed in triplicate with the cell-off and cell-on analyses conducted alternatively. Two adjacent LC injections for cell-off and cell-on analyses were compared to determine the oxidation yield for each run. The measured amount of PEP2 on average of the triplicate measurement is 77.8 pmol, which deviated by 3.8% from the theoretical amount of 75.0 pmol (Table S1, Supporting Information).

Another glycopeptide **PEP3** was measured using the same CMS approach. The +2 ion of **PEP3** was observed at m/z 671.3 before electrolysis. Upon application of a 1.05 V oxidation potential, the +2 ion of the oxidized **PEP3** product was observed at m/z 670.3 (Figures S4a and S4b, Supporting Information). Figures S4c and S4d (Supporting Information) show the EIC

Table 1. List of Tyrosine-Containing Glycopeptides from NIST mAb

Glycan Compositions ^a	Glycoform	CFGb	Peptide Sequence	2+ (<i>m/z</i>)	RT(min)	Average Measured Amount (pmol)
[h3n4f1]	G0F		EEQYNSTYR	1317.52209	25.50	3.34E+01
[h4n3f1]	G1F(-GlcNAc)		EEQYNSTYR	1297.01330	25.86	4.30E+00
[h4n4f1]	G1F		EEQYNSTYR	1398.54883	27.44	3.74E+01
[h5n4f1]	G2F		EEQYNSTYR	1479.57654	29.25	9.32E+00
[h6n4f1]	G2F(Hex)		EEQYNSTYR	1560.60449	30.76	4.28E+00

^a[Glycan Composition]: monosaccharide composition. h = hexose, n = N-acetylhexosamine, f = fucose. ^b[CFG]: Structure using the Consortium for Functional Glycomics (CFG) Notation. Symbol representations of glycans: galactose = yellow circles, mannose = green circles, N-acetylglucosamine = blues boxes, fucose = red triangles.

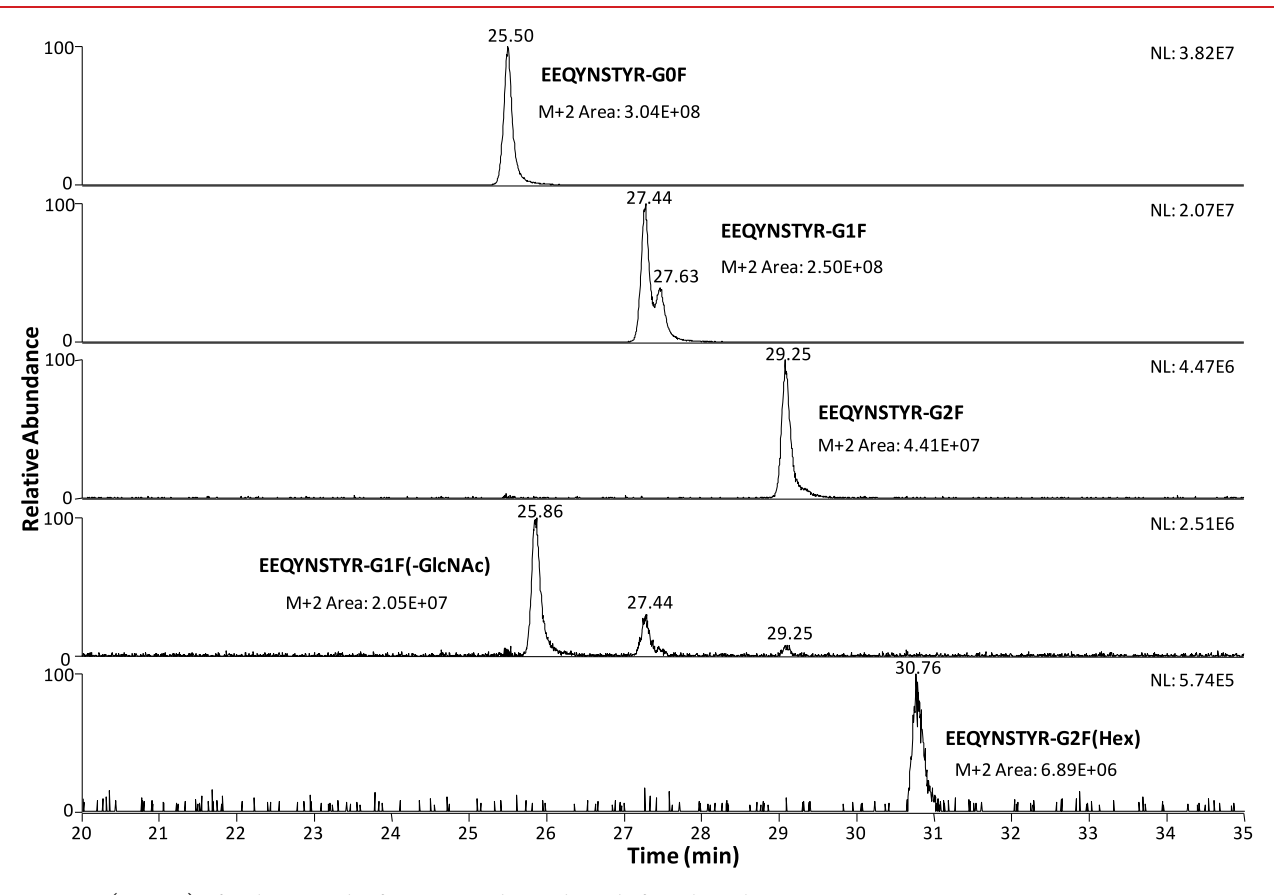


Figure 2. EICs (+2 ions) of 5 glycopeptides from tryptic-digested IgG before electrolysis.

peaks of **PEP3** before and after electrolysis, which showed the oxidation yield to be 61.9% by comparison of the EIC peak area change upon electrolysis. Note that the oxidation efficiencies are dramatically different for glycopeptides **PEP2** and **PEP3** under similar experimental conditions. This could be due to the peptide sequence difference which may influence the electron transfer between the electrode and the peptide and thus affect the peptide oxidation efficiency. Based on the measured electricity *Q*, the amount of oxidized **PEP3** was calculated to be 49.9 pmol and the measured **PEP3** amount was 80.6 pmol

(averaged amount from triplicate measurement = 77.9 pmol; Table S2, Supporting Information). In comparison to the injection amount of 75 pmol, our CMS quantitation error was 3.9%.

Absolute Quantitation of IgG Glycopeptides by CMS.

The most common MS strategy for antibody quantitation in biotherapeutics is a "bottom-up" approach in which a protein is digested into peptides that are more readily ionized and dissociated by MS. Surrogate peptides are selected and quantified by MS. The measured quantity of the surrogate

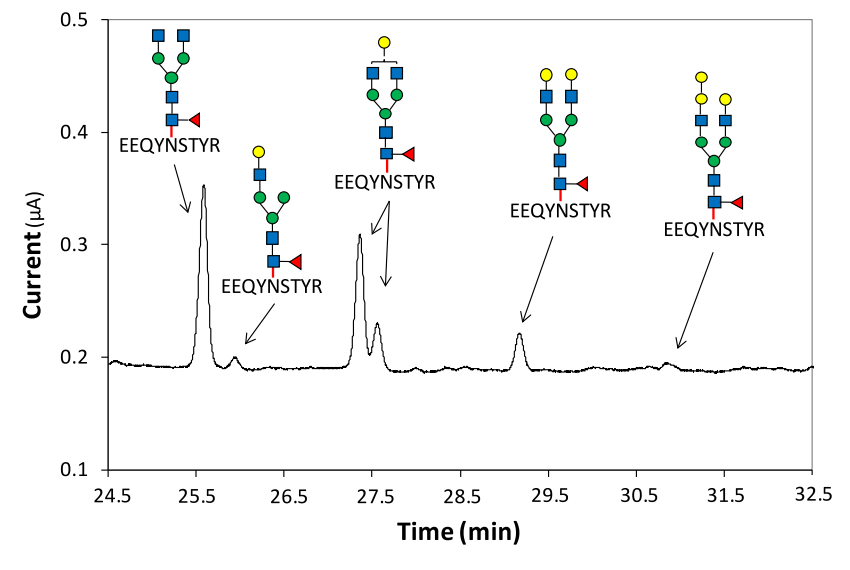


Figure 3. Electric current responses of glycopeptides from IgG digest upon electrochemical oxidation.

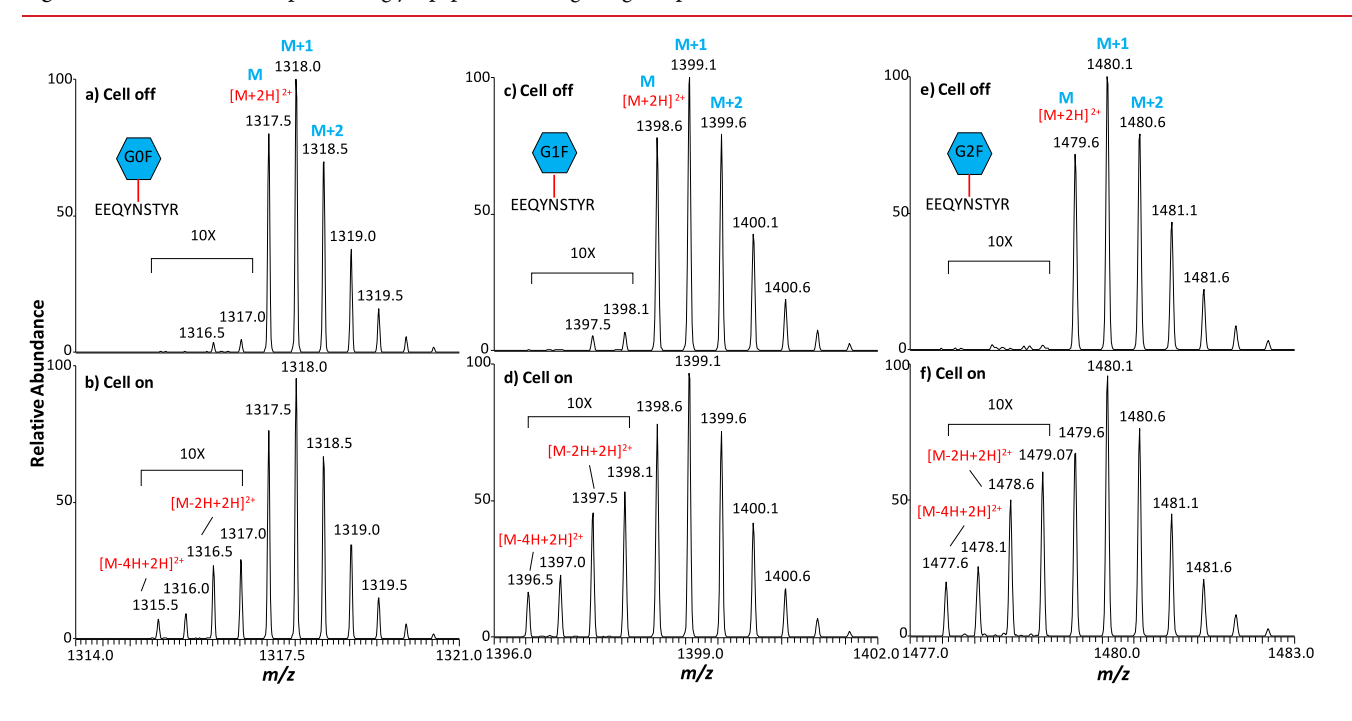


Figure 4. ESI-MS spectra of 3 major glycopeptides from tryptic-digested IgG: EEQYNSTYR-G0F when the applied potentials were (a) 0 and (b) +1.2 V; EEQYNSTYR-G2F when the applied potentials were (e) 0 and (f) +1.2 V.

peptide reflects the amount of protein of interest. We combined the approach of surrogate peptide quantification with our CMS method to achieve standard-free quantitation of surrogate glycopeptides from N297 Fc residue of the heavy chain as well as antibody (Scheme 3). HILIC was chosen to achieve the separation of surrogate glycopeptides due to its retention of hydrophilic substances.⁵⁸

NIST mAb IgG was first trypsin digested. Five tyrosine-containing glycopeptides having a glycan at the N297 Fc residue of the heavy chain, EEQYNSTYR-G0F, EEQYNSTYR-G1F, EEQYNSTYR-G2F, EEQYNSTYR-G1F(-GlcNAc), and EEQYNSTYR-G2F(Hex) (listed in Table 1), where the glycans

attached in the residue of asparagine (N, see the glycopeptide structures in Table 1 and Figure 3) were separated out by a HILIC column with retention times at 25.5, 27.4, 29.3, 25.9, and 30.8 min, respectively (Figure 2). The three major glycoforms observed (based on their EIC intensities shown in Figure 2) were G0F, G1F, and G2F, and the two minor glycoforms are G1F(-GlcNAc) and G2F(hex). Each of these glycopeptides contains two tyrosine residues that can be oxidizable, which are quantified by CMS. As shown in Figure 3, all oxidation current peaks for the five glycopeptides were observed. Notably, EEQYNSTYR-G1F showed a split peak at 27.4 min due to a partial separation of isomeric glycoforms resulting from the

: Glycoform

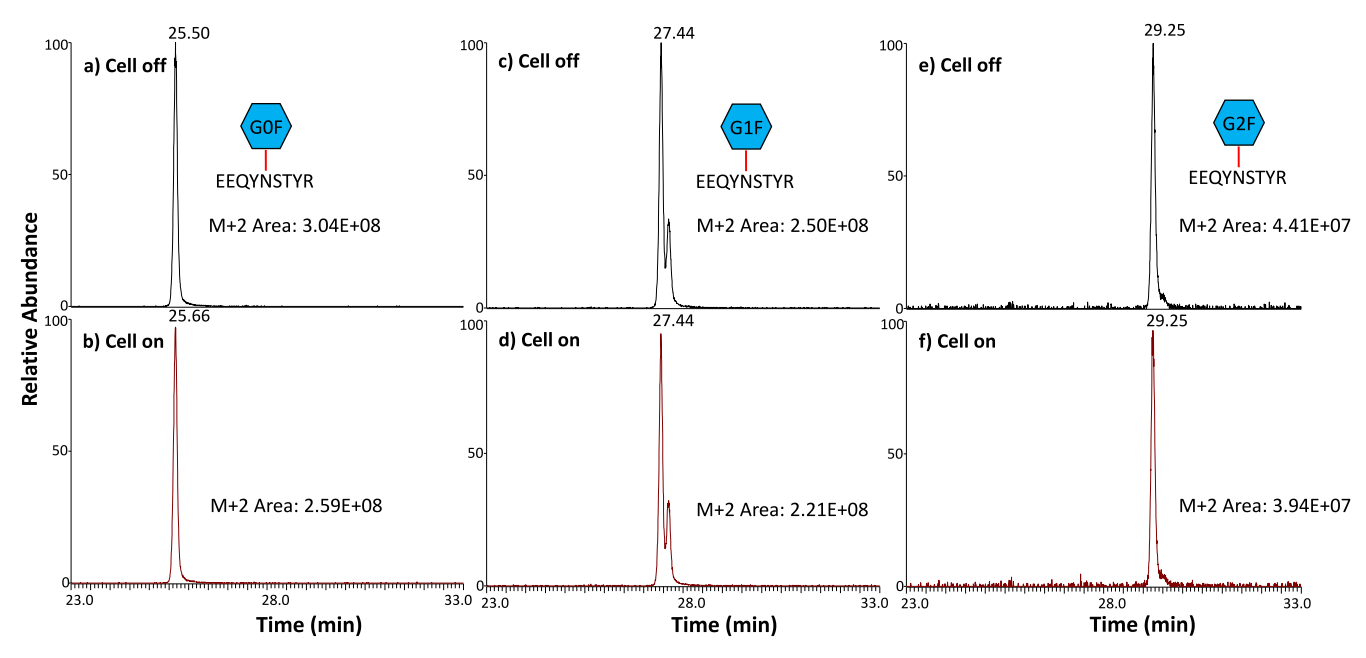


Figure 5. EICs of 3 major glycopeptides from tryptic-digested IgG: EEQYNSTYR-G0F when the applied potentials were (a) 0 and (b) +1.2 V; EEQYNSTYR-G1F when the applied potentials were (c) 0 and (d) +1.2 V; EEQYNSTYR-G2F when the applied potentials were (e) 0 and (f) +1.2 V.

galactose α -3/6 linkage. ⁵⁹ The glycopeptide EEQYNSTYR-G1F(-GlcNAc) eluted out at 25.9 min (see the EIC in the fourth panel of Figure 2), and there are two additional peaks at 27.4 and 29.3 min that were also observed due to the in-source fragmentation of the EEQYNSTYR-G1F and EEQYNSTYR-G2F glycopeptide ions into the EEQYNSTYR-G1F(-GlcNAc) ion.

Furthermore, before electrolysis, the +2 ion of EEQYNSTYR-G0F was observed at m/z 1317.5 (Figure 4a) and a small m/z1316.5 was present, probably due to in-source oxidation of the glycopeptide from the ionization process. After electrolysis, two oxidized products were observed at m/z 1316.5 and 1315.5, corresponding to the oxidation products resulting from one tyrosine oxidation and two tyrosine oxidations, respectively (one tyrosine residue loses two hydrogens and two electrons (z = 2)to form semiquinone upon oxidation; as a result, a 1 Da mass shift occurs to the +2 glycopeptide ion⁴⁶). For CMS quantitation, in terms of the oxidation yield calculation, we chose the third isotope peak (i.e., the M + 2 peak) of m/z 1317.5, which is m/z 1318.5, to avoid interference from the isotopic peaks of the oxidation products. Based on the EIC peak area change of m/z 1318.5 before and after electro-oxidation (Figure 5a and 5b), the oxidation yield for EEQYNSTYR-G0F was found to be 15.0% (Table S3, Supporting Information).

On the other hand, the oxidation current peak of EEQYNSTYR-G0F was detected, as shown in Figure 3. By integration of the current peak area, the total electric charge Q involved in the oxidation was calculated to be 1.22×10^{-6} C, which was via the one tyrosine oxidation pathway ($2 e^-$ per mole peptide toward the formation of m/z 1316.5; z = 2) and via one two-tyrosine oxidation pathway ($4 e^-$ per mole peptide toward the formation of m/z 1315.5; z = 4). In consideration of the similarity of the two structures of the oxidation products, the molar ratio of the two products could be estimated by the peak area ratio. In our previous work, ⁴⁶ we demonstrated the use of this assumption for quantifying one peptide containing two Y residues DRVYIHPFHLLVYS, and the quantitation worked reasonably well (quantitation error was -5.5% The EIC peak

area ratio of m/z 1316.5 to m/z 1315.5 was measured to be 0.701:0.299 (Figure 4 and Table S4, Supporting Information). Note that when we calculated the area ratio of the two oxidation product ions, the third isotopic peak of m/z 1315.5 would overlap with the peak of m/z 1316.5. Hence, the corrected EIC peak area of m/z 1316.5 equals the EIC peak area of m/z 1316.5 where the correction factor α is measured based on the observed ratio of the third isotopic peak to the first isotopic peak for m/z 1317.5. Furthermore, based on Faraday's law

- $Q = 2F \times$ (the moles of the peptide with one tyrosine being oxidized) + $4F \times$ (the moles of the peptide with two tyrosine residues being oxidized)
- = $2F \times$ (the moles of the oxidized peptide \times 0.701) + $4F \times$ (the moles of the oxidized peptide \times 0.299)

Thus, we calculated the amount of the oxidized EEQYN-STYR-G0F to be 4.86 pmol. Considering the oxidation yield of 15.0% as mentioned above, our measured amount of EEQYNSTYR-G0F was therefore 32.4 pmol (Table S3, Supporting Information).

The measurement of EEQYNSTYR-G1F and EEQYNSTYR-G2F followed the same calculation as EEQYNSTYR-G0F, and their averaged quantities from a triplicate measurement were found to be 37.4 and 9.32 pmol, respectively. For EEQYN-STYR-G1F(-GlcNAc) and EEQYNSTYR-G2F(Hex), since there was only one oxidation product (Figure S5, Supporting Information), the calculation followed what was mentioned above for standard glycopeptide PEP3 measurement. Their measured amounts were 4.28 and 4.30 pmol (Table 1), respectively. For this study, the estimated amount of NIST mAb was the sum of all five glycopeptides divided by two as IgG has two identical heavy chains which carry these glycopeptides; the measured IgG amount was 44.4 pmol (Table S3, Supporting Information). Glycopetide abundance was calculated against the

 $Table \ 2. \ Comparison \ of \ Major \ Glycopeptides \ Abundances \ Derived \ from \ NIST \ mAb \ Measured \ by \ CMS \ and \ the \ Reported \ Literature \ Method^{61}$

composition	common name	CMS measurement (pmol)	CMS abundance (%)	Zhao et al. glycopeptide abundance (%) ⁶¹
EEQYNSTYR[h3n4f1]	G0F	3.34×10^{01}	31.5	38.4
EEQYNSTYR[h4n4f1]	G1F	3.74×10^{01}	35.3	34.7
EEQYNSTYR[h5n4f1]	G2F	9.32×10^{00}	8.8	7.4
EEQYNSTYR[h6n4f1]	G2F(Hex)	4.28×10^{00}	4.0	1.7
EEQYNSTYR[h4n3f1]	G1F(-GlcNAc)	4.30×10^{00}	4.1	3.5
total amount %			83.7	85.7

theoretical amount of IgG (10 μ L of the 5.3 μ M IgG, 53.0 pmol); the calculated amount of NIST mAb was close to the theoretical amount. The CMS quantitation error for NIST mAb was -16.2% (Table S3, Supporting Information), likely due to sample loss during protein digestion or the existence of other unmeasured minor glycopeptides.⁶⁰ This result indicates that our CMS result could also be used to estimate the amount of precursor glycoprotein. To show the accuracy of the CMS measurement of glycopeptides, we compared our quantitation results to previous NIST mAb glycosylation studies by Zhao et al.⁶¹ In short, in their work,⁶¹ NIST mAb was trypsin digested and relative quantitation of glycosylated peptides with backbone EEQYNSTYR was based on the peak areas obtained from Thermo Xcalibur Qual Browser. The abundances of glycopeptides were compared with CMS measurement as shown in Table 2. Five glycopeptides measured by CMS have similar abundances to those reported by Zhao et al., which account for 83.7% and 85.7% of the total antibody abundance, respectively. As it can be seen from Table 2, the relative abundances from glycopeptides measured by CMS are close to those measured by Zhao's method,⁶¹ and the difference is that our CMS also provides an absolute quantity for each measured glycopeptide. This result demonstrates the utility of our CMS for glycopeptide quantitation, which suggests the potential good applications of this method for quantitative proteomics. Note that good separation among oxidizable glycopeptides is necessary for our quantitation approach. Currently, there are different types of HILIC columns utilizing different stationary phase modifications that are commercially available. 62 For a very complex sample, we could run fractionation first using one type of HILIC column, and then carry out CMS quantitation of each fraction with another type of HILIC column, so that overlapped glycopeptides (or other oxidizable non-glycosylated peptides) could be separated and become suitable for CMS quantitation.

CONCLUSIONS

In this study, we demonstrated an absolute quantitation strategy for tyrosine-containing glycopeptides by using a coulometric mass spectrometry approach. Standard glycopeptides were successfully quantified by CMS with excellent measurement accuracy. We further applied this method to quantify glycopeptides from digested IgG. Through this approach we were able to precisely estimate the amount of glycoprotein based on the abundance of surrogate glycopeptides. The highlight of CMS is that it does not require an isotope-labeled standard to achieve absolute quantitation, which has the potential to break the bottleneck in many current methods. Furthermore, CMS is likely to be applicable to peptide species that contain other oxidizable residues such as tryptophan, cysteine, and methionine that are typically not considered in a targeted MS approach such as MRM. CMS can also serve as a solution to determine glycosylation site occupancy by quantifying non-glycosylated

peptides. Further work will be focused on applying CMS to other glycoproteins and the improvement of method sensitivity. In addition, we noted that the ion intensities of the observed oxidation product ions relative to the remaining precursor glycopeptide ion (e.g., Figure 4b) appears to be lower than what were expected from the glycopeptide oxidation yield, which may be due to partial adsorption of the oxidation products on the electrode surface. Further effort would also be needed to search for different electrodes or surface-modified electrodes to reduce the potential product adsorption on the electrode surface. A fast and accessible absolute quantitation method like CMS can hugely benefit the study of the influence of glycosylation on therapeutic antibodies in terms of their antigenicity and immunogencity.

ASSOCIATED CONTENT

Supporting Information

The Supporting Information is available free of charge at https://pubs.acs.org/doi/10.1021/jasms.4c00052.

Structures of glycans examined, additional MS data figures, and tables showing calculation results (PDF)

AUTHOR INFORMATION

Corresponding Authors

Harsha P. Gunawardena — The Janssen Pharmaceutical Companies of Johnson & Johnson, Springhouse, Pennsylvania 19002, United States; oorcid.org/0000-0003-3245-3293; Email: hgunawar@ITS.JNJ.com

Hao Chen – Department of Chemistry & Environmental Science, New Jersey Institute of Technology, Newark, New Jersey 07102, United States; ⊚ orcid.org/0000-0001-8090-8593; Email: hao.chen.2@njit.edu

Authors

Kai-Yuan Chiu – Department of Chemistry & Environmental Science, New Jersey Institute of Technology, Newark, New Jersey 07102, United States

Yongling Ai — Department of Chemistry & Environmental Science, New Jersey Institute of Technology, Newark, New Jersey 07102, United States; ⊚ orcid.org/0000-0003-4458-2041

Md Tanim-AI Hassan — Department of Chemistry & Environmental Science, New Jersey Institute of Technology, Newark, New Jersey 07102, United States

Xuanwen Li − Analytical Research & Development, Merck & Co., Inc., Rahway, New Jersey 07065, United States; orcid.org/0000-0001-7548-583X

Complete contact information is available at: https://pubs.acs.org/10.1021/jasms.4c00052

Notes

The authors declare no competing financial interest.

ACKNOWLEDGMENTS

We thank NIH (1R21GM148874-01) and NSF (CHE-2203284) for supporting this work.

REFERENCES

- (1) Uversky, V. N. Posttranslational Modification. In *Brenner's Encyclopedia of Genetics*, 2nd ed.; Maloy, S., Hughes, K., Eds.; Academic Press: San Diego, CA, 2013; pp 425–430.
- (2) Xu, S.; Suttapitugsakul, S.; Tong, M.; Wu, R. Systematic analysis of the impact of phosphorylation and O-GlcNAcylation on protein subcellular localization. *Cell Reports* **2023**, *42* (7), No. 112796.
- (3) Reusch, D.; Haberger, M.; Maier, B.; Maier, M.; Kloseck, R.; Zimmermann, B.; Hook, M.; Szabo, Z.; Tep, S.; Wegstein, J.; Alt, N.; Bulau, P.; Wuhrer, M. Comparison of methods for the analysis of therapeutic immunoglobulin G Fc-glycosylation profiles—part 1: separation-based methods. *MAbs* **2015**, *7* (1), 167–79.
- (4) Kanda, Y.; Yamada, T.; Mori, K.; Okazaki, A.; Inoue, M.; Kitajima-Miyama, K.; Kuni-Kamochi, R.; Nakano, R.; Yano, K.; Kakita, S.; Shitara, K.; Satoh, M. Comparison of biological activity among nonfucosylated therapeutic IgG1 antibodies with three different N-linked Fc oligosaccharides: the high-mannose, hybrid, and complex types. *Glycobiology* **2007**, *17* (1), 104–18.
- (5) Raju, T. S.; Scallon, B. J. Glycosylation in the Fc domain of IgG increases resistance to proteolytic cleavage by papain. *Biochem. Biophys. Res. Commun.* **2006**, 341 (3), 797–803.
- (6) Chandler, K. B.; Leon, D. R.; Kuang, J.; Meyer, R. D.; Rahimi, N.; Costello, C. E. N-Glycosylation regulates ligand-dependent activation and signaling of vascular endothelial growth factor receptor 2 (VEGFR2). *J. Biol. Chem.* **2019**, 294 (35), 13117–13130.
- (7) Seyrek, K.; Richter, M.; Lavrik, I. N. Decoding the sweet regulation of apoptosis: the role of glycosylation and galectins in apoptotic signaling pathways. *Cell Death & Differentiation* **2019**, *26* (6), 981–993.
- (8) Perkey, E.; Maurice De Sousa, D.; Carrington, L.; Chung, J.; Dils, A.; Granadier, D.; Koch, U.; Radtke, F.; Ludewig, B.; Blazar, B. R.; Siebel, C. W.; Brennan, T. V.; Nolz, J.; Labrecque, N.; Maillard, I. GCNT1-Mediated O-Glycosylation of the Sialomucin CD43 Is a Sensitive Indicator of Notch Signaling in Activated T Cells. *J. Immunol* 2020, 204 (6), 1674–1688.
- (9) Matsubara, N.; Imamura, A.; Yonemizu, T.; Akatsu, C.; Yang, H.; Ueki, A.; Watanabe, N.; Abdu-Allah, H.; Numoto, N.; Takematsu, H.; Kitazume, S.; Tedder, T. F.; Marth, J. D.; Ito, N.; Ando, H.; Ishida, H.; Kiso, M.; Tsubata, T. CD22-Binding Synthetic Sialosides Regulate B Lymphocyte Proliferation Through CD22 Ligand-Dependent and Independent Pathways, and Enhance Antibody Production in Mice. *Front. Immunol.* 2018, 9, 820.
- (10) Kuai, R.; Sun, X.; Yuan, W.; Ochyl, L. J.; Xu, Y.; Hassani Najafabadi, A.; Scheetz, L.; Yu, M.-Z.; Balwani, I.; Schwendeman, A.; Moon, J. J. Dual TLR agonist nanodiscs as a strong adjuvant system for vaccines and immunotherapy. *J. Controlled Release* **2018**, 282, 131–139.
- (11) Wright, J. N.; Collins, H. E.; Wende, A. R.; Chatham, J. C. O-GlcNAcylation and cardiovascular disease. *Biochem. Soc. Trans.* **2017**, 45 (2), 545–553.
- (12) Wang, D.; Hu, X.; Lee, S. H.; Chen, F.; Jiang, K.; Tu, Z.; Liu, Z.; Du, J.; Wang, L.; Yin, C.; Liao, Y.; Shang, H.; Martin, K. A.; Herzog, R. I.; Young, L. H.; Qian, L.; Hwa, J.; Xiang, Y. Diabetes Exacerbates Myocardial Ischemia/Reperfusion Injury by Down-Regulation of MicroRNA and Up-Regulation of O-GlcNAcylation. *JACC: Basic to Translational Science* 2018, 3 (3), 350–362.
- (13) Liljedahl, L.; Pedersen, M. H.; Norlin, J.; McGuire, J. N.; James, P. N-glycosylation proteome enrichment analysis in kidney reveals differences between diabetic mouse models. *Clinical Proteomics* **2016**, 13 (1), 22.
- (14) Kunzke, T.; Balluff, B.; Feuchtinger, A.; Buck, A.; Langer, R.; Luber, B.; Lordick, F.; Zitzelsberger, H.; Aichler, M.; Walch, A. Native glycan fragments detected by MALDI-FT-ICR mass spectrometry

- imaging impact gastric cancer biology and patient outcome. *Oncotarget* **2017**, *8* (40), 68012.
- (15) Dings, R. P. M.; Miller, M. C.; Griffin, R. J.; Mayo, K. H. Galectins as Molecular Targets for Therapeutic Intervention. *International Journal of Molecular Sciences* **2018**, *19* (3), 905.
- (16) West, C. A.; Wang, M.; Herrera, H.; Liang, H.; Black, A.; Angel, P. M.; Drake, R. R.; Mehta, A. S. N-Linked Glycan Branching and Fucosylation Are Increased Directly in Hcc Tissue As Determined through in Situ Glycan Imaging. *J. Proteome Res.* **2018**, *17* (10), 3454–3462.
- (17) Tsai, C. H.; Tzeng, S. F.; Chao, T. K.; Tsai, C. Y.; Yang, Y. C.; Lee, M. T.; Hwang, J. J.; Chou, Y. C.; Tsai, M. H.; Cha, T. L.; Hsiao, P. W. Metastatic Progression of Prostate Cancer Is Mediated by Autonomous Binding of Galectin-4-O-Glycan to Cancer Cells. *Cancer Res.* **2016**, *76* (19), 5756–5767.
- (18) Arnold, J. N.; Wormald, M. R.; Sim, R. B.; Rudd, P. M.; Dwek, R. A. The Impact of Glycosylation on the Biological Function and Structure of Human Immunoglobulins. *Annu. Rev. Immunol.* **2007**, 25 (1), 21–50.
- (19) Zhu, Z.; Go, E. P.; Desaire, H. Absolute quantitation of glycosylation site occupancy using isotopically labeled standards and LC-MS. *J. Am. Soc. Mass Spectrom.* **2014**, 25 (6), 1012–1017.
- (20) Palmisano, G.; Melo-Braga, M. N.; Engholm-Keller, K.; Parker, B. L.; Larsen, M. R. Chemical deamidation: a common pitfall in large-scale N-linked glycoproteomic mass spectrometry-based analyses. *J. Proteome Res.* **2012**, *11* (3), 1949–57.
- (21) Choi, B.-K.; Warburton, S.; Lin, H.; Patel, R.; Boldogh, I.; Meehl, M.; d'Anjou, M.; Pon, L.; Stadheim, T. A.; Sethuraman, N. Improvement of N-glycan site occupancy of therapeutic glycoproteins produced in Pichia pastoris. *Appl. Microbiol. Biotechnol.* **2012**, 95 (3), 671–682.
- (22) Li, X.; Li, D.; Pang, X.; Yang, G.; Deeg, H. J.; Guan, F. Quantitative analysis of glycans, related genes, and proteins in two human bone marrow stromal cell lines using an integrated strategy. *Exp Hematol* **2015**, 43 (9), 760.
- (23) Peng, W.; Zhao, J.; Dong, X.; Banazadeh, A.; Huang, Y.; Hussien, A.; Mechref, Y. Clinical application of quantitative glycomics. *Expert review of proteomics* **2018**, *15* (12), 1007–1031.
- (24) de Leoz, M. L.; Young, L. J.; An, H. J.; Kronewitter, S. R.; Kim, J.; Miyamoto, S.; Borowsky, A. D.; Chew, H. K.; Lebrilla, C. B. Highmannose glycans are elevated during breast cancer progression. *Mol. Cell Proteomics* **2011**, *10* (1), No. M110.002717.
- (25) Yu, A.; Zhao, J.; Peng, W.; Banazadeh, A.; Williamson, S. D.; Goli, M.; Huang, Y.; Mechref, Y. Advances in mass spectrometry-based glycoproteomics. *Electrophoresis* **2018**, *39* (24), 3104–3122.
- (26) Wei, J.; Tang, Y.; Bai, Y.; Zaia, J.; Costello, C. E.; Hong, P.; Lin, C. Toward Automatic and Comprehensive Glycan Characterization by Online PGC-LC-EED MS/MS. *Anal. Chem.* **2020**, 92 (1), 782–791.
- (27) Wiśniewski, J. R.; Zougman, A.; Nagaraj, N.; Mann, M. Universal sample preparation method for proteome analysis. *Nat. Methods* **2009**, *6* (5), 359–362.
- (28) Ma, M.; Li, M.; Zhu, Y.; Zhao, Y.; Wu, F.; Wang, Z.; Feng, Y.; Chiang, H.-Y.; Patankar, M. S.; Chang, C.; Li, L. 6-Plex mdSUGAR Isobaric-Labeling Guide Fingerprint Embedding for Glycomics Analysis. *Anal. Chem.* **2023**, 95 (48), 17637–17645.
- (29) Li, M.; Zhong, X.; Feng, Y.; Li, L. Novel Isobaric Tagging Reagent Enabled Multiplex Quantitative Glycoproteomics via Electron-Transfer/Higher-Energy Collisional Dissociation (EThcD) Mass Spectrometry. J. Am. Soc. Mass Spectrom. 2022, 33 (10), 1874–1882.
- (30) Totten, S. M.; Feasley, C. L.; Bermudez, A.; Pitteri, S. J. Parallel Comparison of N-Linked Glycopeptide Enrichment Techniques Reveals Extensive Glycoproteomic Analysis of Plasma Enabled by SAX-ERLIC. J. Proteome Res. 2017, 16 (3), 1249–1260.
- (31) Selman, M. H. J.; Hemayatkar, M.; Deelder, A. M.; Wuhrer, M. Cotton HILIC SPE Microtips for Microscale Purification and Enrichment of Glycans and Glycopeptides. *Anal. Chem.* **2011**, *83* (7), 2492–2499.
- (32) Zhu, R.; Song, E.; Hussein, A.; Kobeissy, F. H.; Mechref, Y. Glycoproteins Enrichment and LC-MS/MS Glycoproteomics in

- Central Nervous System Applications. Methods in molecular biology (Clifton, N.J.) 2017, 1598, 213–227.
- (33) Xu, S.; Yin, K.; Wu, R. Combining Selective Enrichment and a Boosting Approach to Globally and Site-Specifically Characterize Protein Co-translational O-GlcNAcylation. *Anal. Chem.* **2023**, 95 (9), 4371–4380.
- (34) Wang, D.; Huang, J.; Zhang, H.; Ma, M.; Xu, M.; Cui, Y.; Shi, X.; Li, L. ATP-Coated Dual-Functionalized Titanium(IV) IMAC Material for Simultaneous Enrichment and Separation of Glycopeptides and Phosphopeptides. *J. Proteome Res.* **2023**, *22* (6), 2044–2054.
- (35) Stavenhagen, K.; Hinneburg, H.; Thaysen-Andersen, M.; Hartmann, L.; Silva, D. V.; Fuchser, J.; Kaspar, S.; Rapp, E.; Seeberger, P. H.; Kolarich, D. Quantitative mapping of glycoprotein micro-heterogeneity and macro-heterogeneity: an evaluation of mass spectrometry signal strengths using synthetic peptides and glycopeptides. *Journal of Mass Spectrometry* **2013**, 48 (6), 627–639.
- (36) Pabst, M.; Benešová, I.; Fagerer, S.; Jacobsen, M.; Eyer, K.; Schmidt, G.; Steinhoff, R.; Krismer, J.; Wahl, F.; Preisler, J.; Zenobi, R. Differential isotope labeling of glycopeptides for accurate determination of differences in the site-specific glycosylation. *J. Proteome Res.* **2016**, *15*, 326.
- (37) Ross, P. L.; Huang, Y. N.; Marchese, J. N.; Williamson, B.; Parker, K.; Hattan, S.; Khainovski, N.; Pillai, S.; Dey, S.; Daniels, S.; Purkayastha, S.; Juhasz, P.; Martin, S.; Bartlet-Jones, M.; He, F.; Jacobson, A.; Pappin, D. J. Multiplexed protein quantitation in Saccharomyces cerevisiae using amine-reactive isobaric tagging reagents. *Mol. Cell Proteomics* **2004**, *3* (12), 1154–69.
- (38) Ong, S. E.; Blagoev, B.; Kratchmarova, I.; Kristensen, D. B.; Steen, H.; Pandey, A.; Mann, M. Stable isotope labeling by amino acids in cell culture, SILAC, as a simple and accurate approach to expression proteomics. *Mol. Cell Proteomics* **2002**, *1* (5), 376–86.
- (39) Mirgorodskaya, O. A.; Kozmin, Y. P.; Titov, M. I.; Körner, R.; Sönksen, C. P.; Roepstorff, P. Quantitation of peptides and proteins by matrix-assisted laser desorption/ionization mass spectrometry using (18)O-labeled internal standards. *Rapid Commun. Mass Spectrom.* **2000**, *14* (14), 1226–32.
- (40) Anderson, L.; Hunter, C. L. Quantitative mass spectrometric multiple reaction monitoring assays for major plasma proteins. *Mol. Cell Proteomics* **2006**, *5* (4), 573–88.
- (41) Hong, Q.; Lebrilla, C. B.; Miyamoto, S.; Ruhaak, L. R. Absolute quantitation of immunoglobulin G and its glycoforms using multiple reaction monitoring. *Anal. Chem.* **2013**, *85* (18), 8585–93.
- (42) Chen, Z.; Yu, Q.; Yu, Q.; Johnson, J.; Shipman, R.; Zhong, X.; Huang, J.; Asthana, S.; Carlsson, C.; Okonkwo, O.; Li, L. In-depth Sitespecific Analysis of N-glycoproteome in Human Cerebrospinal Fluid and Glycosylation Landscape Changes in Alzheimer's Disease. *Mol. Cell. Proteomics* **2021**, *20*, 100081.
- (43) Sinha, S.; Pipes, G.; Topp, E. M.; Bondarenko, P. V.; Treuheit, M. J.; Gadgil, H. S. Comparison of LC and LC/MS Methods for Quantifying N-Glycosylation in Recombinant IgGs. *J. Am. Soc. Mass Spectrom.* **2008**, *19* (11), 1643–1654.
- (44) Kim, K. H.; Lee, S. Y.; Kim, D. G.; Lee, S.-Y.; Kim, J. Y.; Yoo, J. S. Absolute Quantification of N-Glycosylation of Alpha-Fetoprotein Using Parallel Reaction Monitoring with Stable Isotope-Labeled N-Glycopeptide as an Internal Standard. *Anal. Chem.* **2020**, 92 (18), 12588–12595.
- (45) Cao, C.; Yu, L.; Fu, D.; Yuan, J.; Liang, X. Absolute quantitation of high abundant Fc-glycopeptides from human serum IgG-1. *Anal. Chim. Acta* **2020**, *1102*, 130–139.
- (46) Zhao, P.; Zare, R. N.; Chen, H. Absolute Quantitation of Oxidizable Peptides by Coulometric Mass Spectrometry. *J. Am. Soc. Mass Spectrom.* **2019**, 30 (11), 2398–2407.
- (47) Xu, C.; Zheng, Q.; Zhao, P.; Paterson, J.; Chen, H. A New Quantification Method Using Electrochemical Mass Spectrometry. J. Am. Soc. Mass Spectrom. 2019, 30 (4), 685–693.
- (48) Zhao, P.; Guo, Y.; Dewald, H. D.; Chen, H. Improvements for absolute quantitation using electrochemical mass spectrometry. *Int. J. Mass Spectrom.* **2019**, *443*, 41–45.

- (49) Song, X.; Chen, H.; Zare, R. N. Coulometry-assisted quantitation in spray ionization mass spectrometry. *J. Mass Spectrom.* **2021**, *56* (4), No. e4628.
- (50) Zhao, P.; Wang, Q.; Kaur, M.; Kim, Y.-I.; Dewald, H. D.; Mozziconacci, O.; Liu, Y.; Chen, H. Absolute Quantitation of Proteins by Coulometric Mass Spectrometry. *Anal. Chem.* **2020**, 92 (11), 7877–7883
- (51) Ai, Y.; Zhao, P.; Fnu, P. I. J.; Chen, H. Absolute Quantitation of Tryptophan-Containing Peptides and Amyloid β -Peptide Fragments by Coulometric Mass Spectrometry. *J. Am. Soc. Mass Spectrom.* **2021**, 32 (7), 1771–1779.
- (52) Ai, Y.; Gunawardena, H. P.; Li, X.; Kim, Y. I.; Dewald, H. D.; Chen, H. Standard-Free Absolute Quantitation of Antibody Deamidation Degradation and Host Cell Proteins by Coulometric Mass Spectrometry. *Anal. Chem.* **2022**, *94* (36), 12490–12499.
- (53) Fnu, P. I. J.; Hassan, M. T.-A.; Yaroshuk, T.; Ai, Y.; Chen, H. Absolute quantitation of peptides and proteins by coulometric mass spectrometry after derivatization. *Int. J. Mass Spectrom.* **2024**, 495, No. 117153.
- (54) Wang, Q.; Liu, Z.; Liu, Y.; Chen, H. Absolute Quantitation of N-Nitrosamines by Coulometric Mass Spectrometry without Using Standards. J. Am. Soc. Mass Spectrom. 2022, 33 (5), 875–884.
- (55) Dechtrirat, D.; Gajovic-Eichelmann, N.; Wojcik, F.; Hartmann, L.; Bier, F. F.; Scheller, F. W. Electrochemical displacement sensor based on ferrocene boronic acid tracer and immobilized glycan for saccharide binding proteins and E. coli. *Biosens. Bioelectron.* **2014**, 58, 1–8
- (56) Li, H.; Ortiz, R.; Tran, L.; Hall, M.; Spahr, C.; Walker, K.; Laudemann, J.; Miller, S.; Salimi-Moosavi, H.; Lee, J. W. General LC-MS/MS Method Approach to Quantify Therapeutic Monoclonal Antibodies Using a Common Whole Antibody Internal Standard with Application to Preclinical Studies. *Anal. Chem.* **2012**, 84 (3), 1267–1273
- (57) Picotti, P.; Aebersold, R. Selected reaction monitoring—based proteomics: workflows, potential, pitfalls and future directions. *Nat. Methods* **2012**, 9 (6), 555–566.
- (58) Qing, G.; Yan, J.; He, X.; Li, X.; Liang, X. Recent advances in hydrophilic interaction liquid interaction chromatography materials for glycopeptide enrichment and glycan separation. *TrAC Trends in Analytical Chemistry* **2020**, 124, No. 115570.
- (59) Huang, Y.; Nie, Y.; Boyes, B.; Orlando, R. Resolving Isomeric Glycopeptide Glycoforms with Hydrophilic Interaction Chromatography (HILIC). *Journal of biomolecular techniques: JBT* **2016**, *27* (3), 98–104.
- (60) Lowenthal, M. S.; Liang, Y.; Phinney, K. W.; Stein, S. E. Quantitative Bottom-Up Proteomics Depends on Digestion Conditions. *Anal. Chem.* **2014**, *86* (1), 551–558.
- (61) Zhao, J.; Peng, W.; Dong, X.; Mechref, Y. Analysis of NIST Monoclonal Antibody Reference Material Glycosylation Using the LC-MS/MS-Based Glycoproteomic Approach. *J. Proteome Res.* **2021**, *20* (1), 818–830.
- (62) Molnarova, K.; Duris, A.; Jecmen, T.; Kozlik, P. Comparison of human IgG glycopeptides separation using mixed-mode hydrophilic interaction/ion-exchange liquid chromatography and reversed-phase mode. *Anal. Bioanal. Chem.* **2021**, *413* (16), 4321–4328.